

Dynamic scattering from solutions of semiflexible polymers

Klaus Kroy and Erwin Frey

*Institut für Theoretische Physik, Physik-Department der Technischen Universität München,
James-Frank-Straße, D-85747 Garching, Germany*

(submitted to PRE)

The dynamic structure factor of semiflexible polymers in solution is derived from the wormlike chain model. Special attention is paid to the rigid constraint of an inextensible contour and to the hydrodynamic interactions. For the cases of dilute and semidilute solutions exact expressions for the initial slope are obtained. When the hydrodynamic interaction is treated on the level of a renormalized friction coefficient, the decay of the structure factor due to the structural relaxation obeys a stretched exponential law in agreement with experiments on actin. We show how the characteristic parameters of the system (the persistence length ℓ_p , the lateral diameter a of the molecules, and the mesh size ξ_m of the network) are readily determined by a single scattering experiment with scattering wavelength λ obeying $a \ll \lambda \ll \ell_p$ and $\lambda < \xi_m$. We also find an exact explicit expression for the effective (wave-vector-dependent) dynamic exponent $z(k) < 3$ for semiflexible polymers and thus an enlightening explanation for a longstanding puzzle in polymer physics.

PACS numbers: 61.25.Hq, 87.15.He, 36.20.Ey

I. INTRODUCTION

Recently, there has been increasing interest in biological materials research [1]. The physical properties of colloids, liquid crystals, and macromolecular networks are of prime importance for the structure and function of biological entities such as cells and muscles. On the other hand, biology provides physicists with some of the most pertinent model systems to test their theories of soft matter. Among these systems we will concentrate on solutions of semiflexible macromolecules here. The challenging problems associated with semiflexibility, which have been attacked by numerous groups over many years, have received recent attention. *Semiflexibility* has been recognized as a crucial property for the understanding of many peculiar features of DNA [2,3] and actin [4–8]. This may not be too surprising in the case of actin, which polymerizes into filaments that are rarely much longer than their persistence length. It is perhaps less obvious for DNA molecules, which are typically orders of magnitude longer than their persistence length and thus have an overall flexible appearance.

In this paper we will concentrate on the *dynamic* aspects of semiflexibility. In contrast to the dynamics of flexible polymers [9] the dynamic properties of semiflexible polymers are still not very well understood: Whereas a simple, analytically tractable basic model for flexible polymers has been known for a long time, we lack such a generally accepted simple model in the case of semiflexible polymers. It seems worth mentioning the reason for simplicity and complexity in both cases. The standard model for the statics and dynamics of a flexible polymer is the Gaussian chain [9], which represents the connection of the monomers by an isotropic harmonic potential characterized by a single parameter, the mean square end-to-end distance of the polymer. This description re-

produces many of the universal large scale properties of flexible polymers, which are purely entropic in origin. The universality may be understood as a consequence of the central limit theorem. The harmonic theory allows extensions to nonideal problems by perturbation theory. The simplicity of the model is due to the fractal structure of the Gaussian chain: it looks exactly the same on all scales. This property is clearly not shared by real polymers. They are coiled on large scales, but they are rodlike on length scales below their persistence length ℓ_p . A more realistic polymer model than the Gaussian chain is the so-called “*Kratky-Porod*” model [10]. In this model the conformation is derived from an effective free energy [11],

$$E(\{\mathbf{r}_s\}) = \frac{\kappa}{2} \int_0^L ds \left(\frac{\partial^2 \mathbf{r}_s}{\partial s^2} \right)^2, \quad (1.1)$$

which takes into account the energy cost of *bending* the contour. This is the contour integral over the square of the local curvature multiplied by the bending modulus κ . The conformation resulting from the above free energy together with the rigid constraint $|\partial \mathbf{r}_s / \partial s| = 1$ of an *inextensible contour* is known as the “*wormlike chain*”. It is not a fractal as for the Gaussian chain model but a differentiable curve, which is indeed rodlike on short distances and coiled on large scales. Short and long distances are measured with respect to the decay length of the tangent-tangent correlations, the persistence length $\ell_p = \kappa / k_B T$ [12].

If one does not look for a description of the specific microscopic details of a macromolecule but wants to understand global universal properties, shared by large classes of molecules, then one need not worry about the microscopic discrepancy between a real polymer and the Gaussian chain model in the case of proper flexible polymers

with ℓ_p of the order of the lateral diameter a . In this case the local rodlike structure is part of the nonuniversal microscopic details. However, ℓ_p/a is somewhat larger than 1 in several important cases, e.g., for polystyrene, DNA, actin etc. (for actin $\ell_p/a \simeq 10^3$). One may still hope that the intrinsic stiffness is negligible, when the total contour length L of the molecules is much larger than ℓ_p , because the large scale properties are then dominated by the coil structure.

As far as the dynamics is concerned, this heuristic argument has one flaw with possibly serious consequences: *hydrodynamic interactions* play a crucial role for the dynamic properties of polymers in solution, as they do for any system of Brownian particles in hydrodynamic solvents. Because the dynamics of the solvent, which mediates these interactions, is usually much faster than the Brownian dynamics, the hydrodynamic interactions in dilute and semidilute solutions can be subsumed into an (instantaneous) mobility matrix,

$$\mathbf{H}(\mathbf{r}) = \frac{1}{8\pi\eta r} \left(\mathbf{1} + \frac{\mathbf{r}\mathbf{r}}{r^2} \right), \quad (1.2)$$

called the *Oseen tensor*, which is calculated from the Navier-Stokes equation for the pure solvent [9]. Multiplied by a force acting at the origin it gives a contribution to the velocity \mathbf{v} of the solvent at any point in space \mathbf{r} . This velocity field has the characteristic feature to decay like $1/r$ in real space, where r is the length of the vector \mathbf{r} ; i.e., it is both long ranged and singular at the origin. Physically speaking, the singularity is a consequence of idealizing a physical particle as a mass point and has to be cut off at about the diameter a of the polymer. For a real polymer, this short distance divergence has the consequence that its local semiflexible structure, which one would possibly prefer to neglect, may markedly pronounce itself in the dynamic properties, even if the polymer as a whole looks rather flexible. If one decides to take care of this effect, one immediately runs into a problem: The longitudinal degree of freedom of any contour element of the polymer is suppressed by the presence of its neighboring contour elements. This rigid constraint of a locally inextensible contour is the source of the difficulty in modeling the dynamics of (intrinsically) semiflexible polymers. It renders awkward any general theory [11,13,14] which tries to represent this property faithfully. On the other hand, models that relax the constraint too much — as e.g., the so-called Harris-Hearst-Beals model [15] and its latest descendants [16–19] — include artificial stretching modes and find a Gaussian distribution for all spatial distances along the contour; i.e., the essence of semiflexibility has obviously been lost. The correct radial distribution function of a semiflexible polymer with $L \approx \ell_p$ is actually very different from a Gaussian distribution [20]. It is not peaked at the origin and hence cannot be approximated by a Gaussian form. Moreover, these “Gaussian” models treat the thermal fluctuations to be isotropic. However, as was pointed out by many

workers in the field (see, e.g., Refs. [14,21]), it is conceptually important to be aware of the *local anisotropy* of the bending undulations caused by the rigid constraint of constant contour length.

There is a special case, where semiflexible dynamics can be treated analytically with moderate expense. This is the limit of a *weakly bending rod*, which also has been addressed previously [21–23]. However, these workers did not arrive at the results given below. Especially the crucial point of the local anisotropy of the undulations, which was recognized in Ref. [21] but not discussed in Ref. [23], will be analyzed more closely in this contribution. We will show that this complication does not necessarily prevent an analytical approach. In a forthcoming publication [24] we will also give a quantitative comparison of our results for the decay of the structure factor with new experimental data.

Below, we will demonstrate how one can incorporate the rather complex hydrodynamic interactions and effects from chemical cross-linking in a semidilute solution into the description on a reasonable level of accuracy. To be specific, for the computation of the dynamic structure factor we require the scale separation

$$a \ll \lambda \ll \ell_p, L \text{ and } \lambda < \xi_m \quad (1.3)$$

to be realized. Here we have introduced the symbol ξ_m for the mesh size in a semidilute solution and the scattering wavelength $\lambda = 2\pi/k$. The latter should be shorter than the mesh size to probe the dynamics of *single* polymers. The conditions in Eq. (1.3) are generic for such important cases as neutron scattering or light scattering experiments from semidilute solutions of DNA or actin, respectively.

The outline of the paper is as follows. In Sec. II we derive the functional form of the decay of the dynamic structure factor for semiflexible polymers in solution. Special attention has to be paid to the rigid constraint of constant contour length and to the hydrodynamic interaction. We demonstrate how this can be achieved in the case of interest. We give the exact analytical result for the time decay of the structure factor and show that it can be reduced to a simple stretched exponential law, which is readily applied to determine various parameters of interest from experimental data. In Sec. III we calculate the initial slope of the structure factor. This can be used to measure the microscopic lateral diameter a of the polymer by a dynamic scattering experiment with $\lambda \gg a$. We show that the short time dynamics of semiflexible polymers is characterized by a wavelength-dependent dynamic exponent $z(k)$, which is computed explicitly. What is remarkable about our results compared to other predictions available in the literature [25,21] is that they are simple analytical expressions, which at the same time excellently fit experimental data [6]. Finally, in Sec. IV we summarize our findings and outline some possible experimental applications.

II. STRUCTURAL RELAXATION

For the following we suppose Eq. (1.3) holds. We concentrate on the common case of a semidilute solution, the dilute limit being included as a special case. With the conditions in Eq. (1.3) the decay of the structure factor is mainly caused by the local conformational fluctuations, whereas the global structure of the polymer network stays virtually fixed during the characteristic decay time. This allows for a description of the dynamics purely in terms of the transverse undulations of a weakly bending rod, i.e. in terms of the Langevin equation

$$\frac{\partial}{\partial t} \mathbf{r}_s(t) = \int_0^L ds' \mathbf{H}_\perp(\mathbf{r}_s - \mathbf{r}_{s'}) \left(-\frac{\delta}{\delta \mathbf{r}_{s'}} E(\{\mathbf{r}_{s'}\}) + \tilde{\mathbf{f}}_{s'} \right) \quad (2.1)$$

for the polymer contour \mathbf{r}_s . The random force (per length) $\tilde{\mathbf{f}}_s$ is assumed to represent Gaussian white noise. The conformational energy is given by Eq. (1.1). The mobility matrix

$$\mathbf{H}_\perp(\mathbf{r}) = \frac{e^{-r/\xi_h}}{8\pi\eta r} \left(\mathbf{1} - \frac{|\mathbf{r}\rangle\langle\mathbf{r}|}{r^2} \right) \quad (2.2)$$

serves to mediate the hydrodynamic interaction and to project out the forbidden longitudinal motion of the segments. This is a convenient method to enforce the rigid constraint of fixed contour length mentioned above on the local dynamics. Please note that Eq. (2.2) therefore differs from the Oseen tensor given in Eq. (1.2) by the opposite sign of the projector $|\mathbf{r}\rangle\langle\mathbf{r}|$. Whereas (as a consequence of the incompressibility of the solvent) the longitudinal direction is weighted twice in the usual Oseen tensor, it is now completely suppressed. (Recall that we can neglect the center of mass and rotational modes as a consequence of the time scale separation induced by Eq. (1.3).) The exponential prefactor in Eq. (2.2) accounts for the screening of the hydrodynamic self-interaction of a single molecule by the surrounding network: hydrodynamic interactions over distances longer than the mesh size are largely suppressed because of the larger effective viscosity of the solution as compared to the pure solvent. A formal derivation of the exponential screening term has been achieved before within a self-consistent approach known as the “effective medium theory” [9]. One expects the screening length to be roughly equal to the mesh size. It was indeed shown to obey basically the same scaling law as a function of the concentration [26]. Simple geometrical considerations [27] suggest that the mesh size of a semidilute solution of semiflexible polymers with a large ratio ℓ_p/a obeys to a very good approximation the scaling law

$$\xi_m \propto c^{-1/2}, \quad (2.3)$$

until the mesh size becomes considerably larger than the persistence length.

For the following we will neglect the nonlocal nature of the mobility matrix Eq. (2.2) and replace it by the inverse of the effective transverse friction coefficient (per length)

$$\tilde{\zeta}_\perp = \frac{4\pi\eta}{\ln(\xi_h/a)} \quad (2.4)$$

for the transverse undulations. This coefficient may be obtained from Eq. (2.2) by taking the terms in parentheses in Eq. (2.1) out of the integral and averaging over all segments s for a virtually straight contour. However, we want to point out briefly how one can proceed more rigorously. Working with the full mobility matrix Eq. (2.2) in the equation of motion, Eq. (2.1), one needs its Fourier transform. For the transformation to make sense, the short distance singularity mentioned above has to be cut off at the diameter of the molecule a . For the transverse undulations we thus set the transverse mobility equal to the prefactor in Eq. (2.2) with a short distance cutoff represented by another exponential screening term:

$$H_\perp(r) = \frac{e^{-r/\xi_h} - e^{-r/a}}{8\pi\eta r}. \quad (2.5)$$

This leads to a convenient regularization for the familiar [28,23,25] logarithmic mode number dependence of the hydrodynamic interaction: The Fourier transform of H_\perp is diagonal with the diagonal elements $\tilde{H}_\perp(q)$ given by

$$8\pi\eta\tilde{H}_\perp(q) = \frac{1}{2} \ln \left(\frac{a^{-2} + q^2}{\xi_h^{-2} + q^2} \right) \stackrel{qa \ll 1}{\approx} \frac{1}{2} \ln \left(\frac{a^{-2}}{\xi_h^{-2} + q^2} \right).$$

For modes of wavelength longer than the screening length ($q\xi_h \ll 1$) the last formula reduces to the mode mobility $(2\tilde{\zeta}_\perp)^{-1}$ derived from Eq. (2.6) by the normal mode analysis (see the Appendix), but it predicts a somewhat smaller mobility $\tilde{H}_\perp(q) \rightarrow -\ln qa/8\pi\eta + O((q\xi_h)^{-2})$ for the short wavelength modes with $q\xi_h \gg 1$. It is not a critical approximation to neglect the weak wavelength dependence of the mobility in the following considerations. This will allow for a simple expression for the decay of the structure factor, and at the same time it captures the main effect of the hydrodynamic self-interaction of the single polymers as well as their mutual interaction. The error made in this approximation can in part be compensated by renormalizing ξ_h to an “effective hydrodynamic screening length”. Since the original ξ_h was a phenomenological parameter, which had to be determined from experiment anyway, this is not a serious shortcoming from a practical point of view. For the rather dilute case ($k\xi_m \gg 1$) a theoretical estimate for the parameter ξ_h in Eq. (2.4) — motivated by the exact result, Eq. (3.4), obtained in Sec. III for the initial decay rate — is $k\xi_h = e^{5/6}$ (see the Appendix). A further refinement would be tedious and its effects presumably undetectable in typical scattering experiments.

With the above considerations in mind we may use a “Rouse-like” linear equation with a renormalized friction coefficient $\tilde{\zeta}_\perp$ for the transverse local undulations $\mathbf{r}_s^\perp(t)$:

$$\tilde{\zeta}_\perp \frac{\partial}{\partial t} \mathbf{r}_s^\perp(t) = -\kappa \frac{\partial^4}{\partial s^4} \mathbf{r}_s^\perp(t) + \tilde{\mathbf{f}}_s^\perp. \quad (2.6)$$

The transverse random force (per length) $\tilde{\mathbf{f}}_s^\perp$ represents Gaussian white noise. Eq. (2.6) can be solved by a normal mode analysis. Physically, from Eq. (1.3) one expects that the problem at hand should not depend sensitively on the special choice of the boundary conditions. This may be justified by a formal argument as well. The reader may generally (but not invariably) think of the normal modes as cosine functions (see the Appendix). Effects from chemical cross-linking of the polymers (clamped ends) will be incorporated later on.

To calculate the decay of the dynamic structure factor, we start from the definition

$$g(\mathbf{k}, t) = \frac{1}{N} \sum_{n,m} \langle \exp[i\mathbf{k} \cdot (\mathbf{r}_n(t) - \mathbf{r}_m(0))] \rangle \quad (2.7)$$

for the dynamic structure factor of a statistical system composed of N equal scattering centers (monomers). As we have explained above, our main interest is in situations where the decay of the structure factor is mainly caused by the fast local bending undulations while the global structure of the network stays virtually fixed.

$$g_{nm}(\mathbf{k}, t) := \frac{\exp\left(\frac{\mathcal{R}_{nm}^{\parallel 2}}{\mathcal{R}_{nm}^{\perp 2}(t)} - \frac{k^2 \mathcal{R}_{nm}^{\perp 2}(t)}{4}\right)}{k \mathcal{R}_{nm}^\perp(t)} \left[\operatorname{erf}\left(\frac{i}{2} k \mathcal{R}_{nm}^\perp(t) + \frac{\mathcal{R}_{nm}^\parallel}{\mathcal{R}_{nm}^\perp(t)}\right) + \operatorname{erf}\left(\frac{i}{2} k \mathcal{R}_{nm}^\perp(t) - \frac{\mathcal{R}_{nm}^\parallel}{\mathcal{R}_{nm}^\perp(t)}\right) \right]. \quad (2.10)$$

To proceed further we introduce the Rouse-like decay time of the mode of wavelength $2L$

$$\tau_L = \frac{\tilde{\zeta}_\perp}{\kappa} \left(\frac{L}{\pi}\right)^4, \quad (2.11)$$

which is immediately read off by dimensional analysis from Eq. (2.6) as the characteristic time scale. As another natural abbreviation we introduce the decay rate

$$\gamma_k = \frac{k_B T}{\tilde{\zeta}_\perp} k^{\frac{8}{3}} \ell_p^{-\frac{1}{3}}, \quad (2.12)$$

which will be shown to govern the time decay of the structure factor. The decay rate γ_k may also be predicted by a simple scaling argument [28,23]: For the wormlike chain the amplitudes of small transverse undulations scale as $r^{\perp 2} \propto r^{\parallel 3}/\ell_p$ with the wavelength r^\parallel . Substituting the scattering wavelength λ for the amplitude r^\perp of the undulations and r^\parallel for the contour length parameter L in Eq. (2.11) one obtains Eq. (2.12). This heuristic argument is a special case of a more general theorem derived in Ref. [28] for the dispersion relation of the decay rate:

$$\gamma_k \propto k^{2/\alpha} \quad \text{with} \quad \alpha = \frac{2\zeta}{D + 2\zeta + a},$$

Therefore, we perform the conformational average in two steps: First we take the thermal average $\langle \dots \rangle_T$ over the transverse undulations of a weakly bending rod keeping the mean orientation of the rod fixed in space. Then we average over an isotropic ensemble of rod orientations $\langle \dots \rangle_O$. As the transverse undulations obey a linear Langevin equation, they have Gaussian correlations as the random forces. Using the abbreviations

$$\mathcal{R}_{nm}^\parallel := a(n - m), \quad \mathcal{R}_{nm}^{\perp 2}(t) := \langle (\mathbf{r}_n^\perp(t) - \mathbf{r}_m^\perp(0))^2 \rangle_T$$

we can rewrite $g(\mathbf{k}, t)$ as

$$\frac{1}{N} \sum_{nm} \left\langle \left\langle \exp\left[i\mathbf{k}^\perp \cdot (\mathbf{r}_n^\perp(t) - \mathbf{r}_m^\perp(0))\right] \right\rangle_T \exp[ik^\parallel \mathcal{R}_{nm}^\parallel] \right\rangle_O$$

and, after performing the thermal average, as

$$\frac{1}{N} \sum_{nm} \left\langle \exp\left[-k^{\perp 2} \mathcal{R}_{nm}^{\perp 2}(t)/4\right] \exp[ik^\parallel \mathcal{R}_{nm}^\parallel] \right\rangle_O. \quad (2.8)$$

Performing now also the orientational average, we obtain the explicit general expression

$$g(\mathbf{k}, t) = -\frac{i\sqrt{\pi}}{2N} \sum_{nm} g_{nm}(\mathbf{k}, t), \quad (2.9)$$

with

the stretching exponent. Here ζ denotes the roughness exponent ($\zeta = 3/2$ for the weakly bending rod), D is the dimension of the fluctuating manifold, and a characterizes the hydrodynamic interaction ($a = 0$ in the present case).

After solving Eq. (2.6) by a normal mode analysis and some technical manipulations (see the Appendix) we find

$$k^2 \mathcal{R}_{nm}^{\perp 2}(t) = \frac{4}{\pi} (\gamma_k t)^{\frac{3}{4}} I(x_m, y) + k^2 \mathcal{R}_{nm}^{\perp 2}(0), \quad (2.13)$$

where we have introduced for $t > 0$ the dimensionless variables $x_m := (t/\tau_{L_m})^{1/4}$, $y := k \mathcal{R}_{nm}^\parallel / [(\gamma_k t)^{\frac{1}{4}} (k \ell_p)^{\frac{1}{3}}]$ and [29]

$$I(x_m, y) := \int_{x_m}^{\infty} dx \frac{\cos(xy)}{x^4} (1 - e^{-x^4}). \quad (2.14)$$

The lower limit of the integral serves to exclude modes of wavelength longer than $2L_m$. By L_m we denote the contour length between adjacent clamped points along the contour. This infrared cutoff is a heuristic way to

take into account the effects of steric constraints, so-called entanglements. Strictly speaking, these entanglements cannot fix the polymers in space efficiently at short times ($\mathcal{R}_{nn}^{\perp 2}(t) \ll \xi_m^2$), i.e., until an average contour element has moved a distance of the order of the mesh size ξ_m . Only for times longer than $1/\gamma_{\xi_m}^{-1}$ do the constraints suppress modes of wavelength longer than the entanglement length $L_m = (3/2\xi_m^2\ell_p)^{1/3}$ [30]. However, this subtle point can safely be neglected, because $x_m \ll 1$ for short times ($\gamma_{\xi_m}^{-1}t \ll 1$) anyway. If kL_m is sufficiently large the modes which contribute most to the decay are not substantially disturbed until the structure factor has completely decayed, i.e., $\gamma_k\tau_{L_m} \simeq (k\xi_m)^{8/3} \gg 1$ and we can take the limit $x_m \rightarrow 0$ in Eq. (2.14). On the other hand, if the condition $k\xi_m \gg 1$ is not fulfilled, the steric constraints become important and the structure factor decays in two steps: For short times ($\mathcal{R}_{nn}^{\perp 2}(t) \ll \xi_m^2$) the decay is mainly due to the fast single chain dynamics. As a consequence of the infrared cutoff x_m the structure factor does not decay to zero but only to a value $g(k, t \gg \tau_{L_m})/g(k, 0) \approx \exp[-(\gamma_k\tau_{L_m})^{3/4}/3\pi]$. The further decay is due to the slower collective modes of the network, which are not considered here. An obvious question in this context is how is the single chain dynamics affected by chemical cross-links? It is our opinion the chemical cross-links should *not* be discernible from entanglements by just looking at the single chain dynamics. However, chemical cross-linking often leads to microphase syneresis [31], i.e., to separated microphases with the local mesh size being longer or shorter respectively than the average mesh size. The results derived below can also be applied to investigate such more complex situations [24].

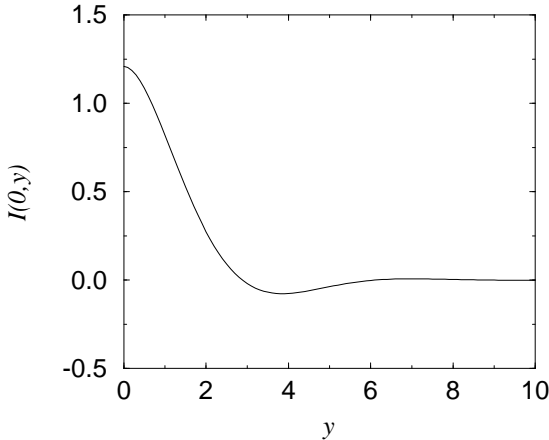


FIG. 1. The function $I(0, y)$ of Eq. (2.14), which appears as a time-dependent prefactor in the approximate scaling law for $k^2\mathcal{R}_{nm}^{\perp 2}(t) - k^2\mathcal{R}_{nm}^{\perp 2}(0)$ in Eq. (2.13).

Let us further discuss Eq. (2.13) for the rather dilute case ($x_m = 0$) without corrections from steric constraints first. Note that for very *short* times ($t \ll (k\ell_p)^{-4/3}\gamma_k^{-1}$) the peaked function $I(0, y)$ of Eq. (2.14) shown in Fig. 1 vanishes for all but the diagonal terms in the sum in

Eq. (2.9). (Because we neglect end effects ($kL \gg 1$) and treat the polymer as homogeneous, we will speak of *the* diagonal term and write $k^2\mathcal{R}_0^{\perp 2}(t) = \frac{4}{\pi}(\gamma_k t)^{\frac{3}{4}}I(0, 0)$ for $k^2\mathcal{R}_{nn}^{\perp 2}(t)$.) As a consequence, the time decay of the structure factor is dominated by the diagonal element(s) of the sum in Eq. (2.9) and we have up to static terms

$$g(\mathbf{k}, t) \propto \sqrt{\pi} \exp\left(-\frac{k^2\mathcal{R}_0^{\perp 2}(t)}{4}\right) \frac{\text{erf}(ik\mathcal{R}_0^{\perp}(t)/2)}{ik\mathcal{R}_0^{\perp}(t)}. \quad (2.15)$$

This differs markedly from a simple exponential by its algebraically slow decay for long times but reduces to

$$g(\mathbf{k}, t) \propto \exp(-k^2\mathcal{R}_0^{\perp 2}(t)/6) \quad (2.16)$$

for the short times $t \ll (k\ell_p)^{-4/3}\gamma_k^{-1}$, where it is supposed to be valid. For comparison, this function together with Eq. (2.15) and Eq. (2.17) is depicted in Fig. 2. We suspect that Eq. (2.16) may not be discernible in experiments, because it belongs to a time regime which falls within the crossover to the simple exponential initial decay, i.e., the time $(k\ell_p)^{-4/3}\gamma_k^{-1} \simeq \tau_{k-1} \simeq \eta/\kappa k^4$ is of the same order of magnitude as the crossover time t^* [33] to the initial decay regime discussed in Sec. III and in the Appendix. On the other hand, for sufficiently *long* times $t \gg (k\ell_p)^{-4/3}\gamma_k^{-1}$ the function $I(0, y)$ may be replaced by the constant $I(0, 0)$, because of the strongly oscillating static terms shown in Fig. 3. Note that in the limit of large $k\ell_p$ “sufficiently long times” may be considerably shorter than the characteristic decay time γ_k^{-1} . Then, we can moreover neglect the static term $\mathcal{R}_{nm}^{\perp 2}(0)$ in Eq. (2.13). Hence, $\mathcal{R}_{nm}^{\perp 2}(t)$ is replaced by $\mathcal{R}_0^{\perp 2}(t)$ for all relevant times, and using the relation $\frac{1}{N} \sum_{nm} \exp(ik^{\parallel}\mathcal{R}_{nm}^{\parallel}) \propto \delta(k^{\parallel})$, Eq. (2.8) reduces again to a simple exponential form

$$g(\mathbf{k}, t) \propto \exp(-k^2\mathcal{R}_0^{\perp 2}(t)/4) \quad (k\ell_p \gg 1). \quad (2.17)$$

The last result also could have been obtained immediately from Eq. (2.8) for a purely transverse scattering geometry with $\mathbf{k} \equiv \mathbf{k}^{\perp}$. This is what one expects, of course, since the longitudinal degree of freedom is suppressed and thus cannot contribute to inelastic scattering. Note that Eq. (2.17) is very similar to what one would have predicted if the rigid constraint of constant contour length had been neglected altogether and isotropic motion of the local contour elements had been assumed. The end result in this approximation is obviously insensitive to the constraint except that the mobility coefficient, which enters the calculation of $\mathcal{R}_0^{\perp 2}(t)$, is reduced as compared to the isotropic model. In other words, except for their different mobility an ensemble of randomly oriented scattering centers, which are constrained to move in two dimensions, cannot be distinguished from an ensemble of isotropically moving scattering centers by their dynamic scattering. This fact inspired us to use a simplified procedure to calculate the initial decay rate in Sec. III. It also explains the fortunate success of some of the “Gaussian” models

in fitting experimental data [19]. Let us emphasize, however, that the reduction of the mobility coefficient due to the anisotropy of the undulations, which the “Gaussian” models fail to account for, is a crucial point that must not be neglected if one wants to obtain quantitative results and gain a real understanding of the underlying physics.

Summarizing the above discussion we conclude that the time decay of the dynamic structure factor for a rather dilute solution ($k\xi_m \gg 1$) of semiflexible polymer obeys

$$g(\mathbf{k}, t) \propto \exp\left(-\frac{\Gamma(\frac{1}{4})}{3\pi}(\gamma_k t)^{\frac{3}{4}}\right). \quad (2.18)$$

(Here we have used $I(0, 0) = \Gamma(1/4)/3$.) For short times $t \ll (k\ell_p)^{-4/3}\gamma_k^{-1}$ we predict a deviation of the functional form of the decay from Eq. (2.18) according to $g(\mathbf{k}, t) \propto \exp(-2\Gamma(\frac{1}{4})/9\pi(\gamma_k t)^{\frac{3}{4}})$ and ultimately to the initial decay law derived in Sec. III.

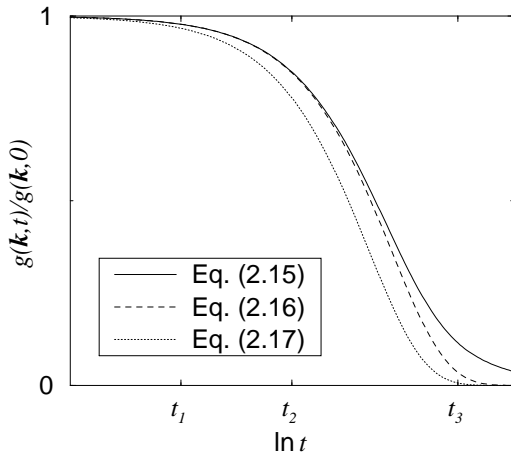


FIG. 2. A comparison of the decay laws Eq. (2.15), Eq. (2.16), and Eq. (2.17) on a logarithmic time scale. Indicated are the times t_i referred to in Figure 3.

A stretched exponential decay as predicted by Eq. (2.18) has indeed been found in several experimental light scattering studies with semidilute actin solutions [23,6]. Assuming that the persistence length of actin is about $17 \mu\text{m}$ [34], we conclude that $k\ell_p \simeq 10^2$ and Eq. (2.18) should be well suited to describe dynamic light scattering from actin solutions. However, some fluorescence microscopy studies [38] suggest that the flexibility of actin could be strongly length scale dependent and that actin may be much more flexible on the characteristic length scales probed in light scattering experiments. According to these results one would estimate $k\ell_p \simeq 10^1$ and expect $g(\mathbf{k}, t)$ to cross over to Eq. (2.16) as discussed after Eq. (2.18).

For the genuinely semidilute case, when $k\xi_m \simeq 1$ and effects from steric constraints are not negligible, we have to consider the infrared cutoff $x_m > 0$ in Eq. (2.14). For $\gamma_k \tau_{L_m} \simeq (k\xi_m)^{8/3}$ of the order of 1 the structure factor

decays in two steps as we have mentioned after Eq. (2.14). We restrict the following analysis to the fast decay due to the single chain dynamics ($t/\tau_{L_m} \equiv x_m^4 < 1$). Then it is useful to split the integral in Eq. (2.14) into two parts, one of which runs from zero to infinity and the other from zero to x_m . A Taylor expansion of the integrand of the second integral renders $k^2 \mathcal{R}_0^\perp(t)$ to order $O(t^2)$ in the simple form

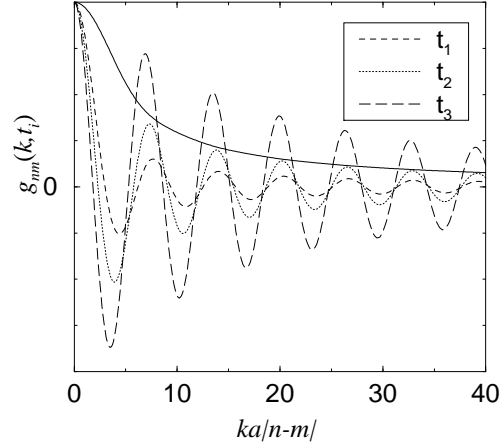


FIG. 3. Static terms suppress contributions to the structure factor which arise from correlations of distant contour elements. For several fixed times t_i indicated in Figure 2, $g_{nm}(k, t)$ from Eq. (2.10) is shown as a function of $k\mathcal{R}_{nm}^\parallel$ in the rod limit, i.e., for infinite persistence length ℓ_p . The oscillations decay more slowly for larger times. For comparison the static structure factor of a rigid rod (solid line) has been included.

$$k^2 \mathcal{R}_0^\perp(t) = \frac{4}{\pi}(\gamma_k t)^{\frac{3}{4}} \left(\frac{\Gamma(\frac{1}{4})}{3} - \left(\frac{t}{\tau_{L_m}} \right)^{\frac{1}{4}} + \frac{1}{10} \left(\frac{t}{\tau_{L_m}} \right)^{\frac{5}{4}} \right).$$

This expression allows one to extract the entanglement length L_m (and thus the mesh size ξ_m) from experimental data and may eventually become useful in understanding the very interesting phenomena [31] that occur when semiflexible polymer solutions are gradually cross-linked. The same perturbation expansion has previously been claimed to account for hydrodynamic screening effects [32]. We do not agree with this interpretation: Hydrodynamic screening reduces the hydrodynamic correlations. Nevertheless, the mobility for the long modes certainly does not decrease to zero but saturates at the finite value $2\tilde{\zeta}_\perp$, as we have shown explicitly by use of Eq. (2.5). See also the discussion after Eq. (2.14).

III. INITIAL SLOPE

The results of the preceding section show that the structure factor $g(\mathbf{k}, t)$ of a solution of semiflexible polymers decays on a characteristic time scale γ_k^{-1} by a stretched exponential law, Eq. (2.18). However, this expression is not valid in the limit $t \rightarrow 0$. The initial slope

of the structure factor does not become infinitely steep. Instead, as we explicitly demonstrate in the Appendix, $g(\mathbf{k}, t \rightarrow 0)$ asymptotically approaches a simple exponential law, $\exp(-\gamma_k^{(0)}t)$ [33]. To calculate the initial decay rate

$$\gamma_k^{(0)} := - \left. \frac{\ln g(\mathbf{k}, t)}{dt} \right|_0 \quad (3.1)$$

of the time decay of the dynamic structure factor we again suppose that Eq. (1.3) is fulfilled. A rigorous scheme for the calculation of the initial slope of the structure factor for an ensemble of beads — coupled by a potential $E(\{\mathbf{r}_s\})$ and by the hydrodynamic interaction — may be found in the textbook of Doi and Edwards [9]. Here we assume that the stiffness of the molecule is not too large, so that the time scale separation between solvent fluctuations and structural relaxation still holds, i.e., the characteristic relaxation rate of a bending undulation of wavelength $(\ell_p \lambda^2)^{1/3}$ is supposed to be much smaller than the characteristic diffusion rate of solvent fluctuations of the same size. Then the hydrodynamically driven small fluctuations about the equilibrium conformation (where the potential forces vanish) are much faster than the structural relaxation of typical bending undulations and hence dominate the short time behavior of the dynamic structure factor. What is special about the case of a semiflexible polymer is again the rigid constraint imposed by the locally rodlike contour.

$$\gamma_k^{(0)} = \frac{k_B T}{2\eta} \int^{1/a} \frac{dq}{(2\pi)^2} \frac{g(q)}{g(k)} \left[\frac{(q^2 - k^2)^2}{2qk\xi_h^{-2}} \ln \left| \frac{q-k}{q+k} \right| + \frac{(q^2 + \xi_h^{-2} - k^2)^2 + 4\xi_h^{-2}k^2}{4qk\xi_h^{-2}} \ln \frac{(q+k)^2 + \xi_h^{-2}}{(q-k)^2 + \xi_h^{-2}} - 1 \right]. \quad (3.3)$$

The static properties of the polymer enter the calculation only via the static structure factor $g(k)$ and through the factor $1/2$. This implies a certain universality of the initial decay rate even in the semiflexible case. However, it turns out to be less universal than predicted by the Gaussian chain model. The main contributions to the integral come from large q . It actually diverges at the upper limit as a consequence of the short distance singularity of the Oseen tensor mentioned in the Introduction. This justifies the weakly bending rod approximation and for $\lambda \ll \ell_p, L$ we may replace the static structure factor by its asymptotic form $g(k) \propto k^{-1}$. Again, we have introduced the lateral diameter a of the molecule to cut off the ultraviolet divergence. After doing the integral and dropping all but the leading order terms in ka one obtains in the dilute limit ($k\xi_h \rightarrow \infty$) the strikingly simple result

$$\gamma_k^{(0)} = \frac{k_B T}{6\pi^2 \eta} k^3 \left(\frac{5}{6} - \ln ka \right). \quad (3.4)$$

Working with the full (rather lengthy) expression may be necessary in some applications, but the conceptual and practical significance of the result is best appreciated in the above limit. The deviation of Eq. (3.4) from

If one would just follow the Doi-Edwards scheme naively, paying regard to the rodlike structure of the molecule only through the static structure factor, the Oseen tensor would render each contour element two times as mobile along the contour as in the transverse directions, thus adding an artificial extra degree of freedom to the weakly bending rod problem, which is moreover weighted twice. On the level of a mere counting of degrees of freedom, one can thus say that — compared to the mobility matrix Eq. (2.2) — this amounts to overestimating the overall mobility of a contour element by a factor of 2. If reversed, this argument tells that one may follow the simple computational scheme of Ref. [9] if the result is divided by two in the end. This is indeed how we will proceed below. Of course, the procedure is not strictly rigorous: it does not pay regard to the local anisotropy of the motion due to the rigid constraint. On the other hand, it takes the local reduction of the degrees of freedom properly into account. From our experience with the problem of local anisotropy in the preceding section we may expect the result to be exact.

Using the screened Oseen tensor in Fourier space,

$$\mathbf{H}(\mathbf{k}) = \frac{1}{\eta(k^2 + \xi_h^{-2})} \left(\mathbf{1} - \frac{|\mathbf{k}\rangle\langle\mathbf{k}|}{k^2} \right), \quad (3.2)$$

we arrive at the following integral for the initial decay rate

the scaling law $\gamma_k^{(0)} \sim k^3$ for a Gaussian chain is weak, hence it is useful to express Eq. (3.4) as a quasiscaling law $\gamma_k^{(0)} \sim k^{z(k)}$ with a wave-vector-dependent dynamical exponent $z(k)$ given by

$$z(k) = 3 \frac{6 \ln ka - 3}{6 \ln ka - 5}. \quad (3.5)$$

This result is depicted in Fig. 4 together with a representative curve for the more complicated semidilute case. It seems to account well for the deviations from the Gaussian chain prediction $z = 3$ seen in several experiments with polystyrene [35]. It is tempting to speculate that these are a signature of hydrodynamically enhanced local semiflexibility. It would be worth checking whether the initial decay of the structure factor measured by neutron scattering from solutions of polystyrene, DNA or any other intrinsically semiflexible polymer may be fitted by Eq. (3.4) with a reasonable value for a . Indeed, in the case of the biopolymer actin Eq. (3.4) already passed this test with remarkable success: It fits excellently available light scattering data with $a = 5.4$ nm [6], which compares very well to the value of 5.16 ± 0.3 nm obtained by much more elaborate methods [36,37] for two times

the transversal radius of gyration of the actin filament. Note that the resolution suggested by this comparison is far beyond the scattering wavelength, which was about an order of magnitude larger than a in the cited light scattering experiments. If the screening length has a finite value, Eq. (3.4) and Eq. (3.5) have to be replaced by more complicated expressions, e.g.,

$$\gamma_k^{(0)} = \frac{k_B T k^3}{180 \eta \pi^2} \left[28 - 30 \ln(ka) + 6 k^{-2} \xi_h^{-2} - 6 k^{-3} \xi_h^{-3} \arctan(k \xi_h) - 30 k^{-1} \xi_h^{-1} \arctan(k \xi_h) - 3 k^2 \xi_h^2 \ln(1 + k^{-2} \xi_h^{-2}) - 15 \ln(1 + k^{-2} \xi_h^{-2}) \right] \quad (3.6)$$

for $k \xi_h \gg 1$, but the qualitative structure is preserved. The main effect of screening is to flatten the increase of $\gamma_k^{(0)}$ and $z(k)$ in the long wavelength limit (cf. Fig. 4). The above results for the dilute case can still be considered a reasonable approximation for semidilute solutions in a restricted range of scattering wavelengths $\lambda \ll \xi_m$.

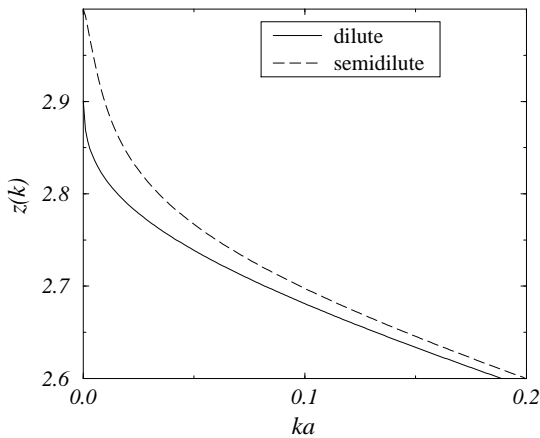


FIG. 4. The effective (wave-vector-dependent) dynamic exponent $z(k)$. The solid line is a plot of Eq. (3.5) for the dilute case. The dashed line is a representative curve for a semidilute solution with screened hydrodynamic interactions ($\xi_h = 200a$).

IV. CONCLUSIONS

Dynamic scattering experiments allow for an accurate measurement of model parameters, if the number of these parameters is small and, of course, if the model is adequate within the range of wavelength and frequency probed. Scattering techniques are then sometimes more convenient than direct methods developed recently to investigate the dynamics of individual polymers, such as flicker analysis [38] and microrheology [39], which are still plagued by some technical complications [40]. They allow to probe in a quick and reliable experiment the internal dynamics of single polymers with the necessary statistical averaging inherently included. It was the purpose

of our work to derive (within the common experimental accuracy) exact analytical expressions for the time decay of the dynamic structure factor for solutions of semiflexible polymers. We succeeded in the case of Eq. (1.3), i.e., for scattering from the internal undulations of genuinely semiflexible polymers in solution. This is a generic situation for neutron scattering from DNA or light scattering from actin solutions, just to mention two outstanding applications. Our analytical results for the initial decay rate and the dynamic exponent for semiflexible polymers suggest that deviations of the dynamic exponent for (more or less) flexible polymers from its classical value $z = 3$ are probably due to the local semiflexible structure of these molecules, and that the above analysis is therefore of some relevance also to scattering from rather flexible polymers. Moreover, these results lead to a convenient method to measure the microscopic lateral diameter a of a semiflexible polymer by use of the simple Eq. (3.4). From a fit of the result for $g(\mathbf{k}, t)/g(\mathbf{k}, 0)$,

$$\exp \left[-\frac{(\gamma_k t)^{\frac{3}{4}}}{\pi} \left(\frac{\Gamma(\frac{1}{4})}{3} - \left(\frac{t}{\tau_{L_m}} \right)^{\frac{1}{4}} + \frac{1}{10} \left(\frac{t}{\tau_{L_m}} \right)^{\frac{5}{4}} \right) \right],$$

valid for $k \ell_p \gg 1$ and intermediate times t

$$(k \ell_p)^{-\frac{4}{3}} \gamma_k^{-1} \ll t \ll \tau_{L_m},$$

to experimental data one finds with good accuracy the bending modulus κ (and the persistence length $\ell_p = \kappa/k_B T$) of the molecules. For $k \xi_m \approx 1$ the mesh size ξ_m and the effective hydrodynamic screening length ξ_h of the network can be determined. In the case of chemical cross-linking one has to be more careful since the development of microphases can cause the mesh size to vary considerably throughout the sample. For sufficiently large $k L_m$ the terms containing τ_{L_m} can be neglected and the dynamic structure factor obeys Eq. (2.18). Note that the hydrodynamic screening length ξ_h is closely related to the mesh size ξ_m , because the surrounding network disturbs the hydrodynamic autocorrelations of the individual polymers over distances longer than ξ_m . However, one should keep in mind that — due to our approximate treatment of the hydrodynamic interaction in Sec. II — ξ_h in the effective friction coefficient used in Sec. II must be regarded as an effective parameter, which will in general differ from ξ_m in its absolute value because it compensates for the deviation of the simple coefficient Eq. (2.2) from a more accurate description as Eq. (2.5). Finally we want to mention a hidden ambiguity of the above results. According to Eqs. (2.3), (2.4), and (2.12) a stiffening of the molecule (e.g., by a chemical manipulation) as well as an increase in concentration may cause a slowing down of the time decay of the structure factor. An apparent increase in concentration may easily be caused by all kinds of syneresis in the course of chemical cross-linking, although the overall concentration remains constant. Therefore some caution is needed in the interpretation of experimental data.

Acknowledgments This work was supported by the Deutsche Forschungsgemeinschaft (DFG) under Contract No. Fr. 850/2 and No. SFB 266. We are grateful to R. Götter, E. Sackmann, M. Fuchs and J. Wilhelm for helpful discussions.

-
- [1] See, e.g., in *Physics of Biomaterials: Fluctuations, Self Assembly and Evolution*, Vol. 322, NATO ASI, edited by T. Riste, and D. Sherrington (Kluwer Academic, Dordrecht, 1995).
- [2] C. Bustamente, J. F. Marco, E. D. Siggia, and S. Smith, *Science* **265**, 1599 (1994); J. F. Marko, and E. D. Siggia, *Macromol.* **28** 8759 (1995).
- [3] R. E. Goldstein and S. A. Langer, *Phys. Rev. Lett.* **75**, 1094 (1995).
- [4] E. Sackmann, *Macromol. Chem. Phys.* **195**, 7 (1994).
- [5] F. C. MacKintosh, J. Käs, and P. A. Janmey, *Phys. Rev. Lett.* **75**, 4425 (1995).
- [6] R. Götter, K. Kroy, E. Frey, M. Bärmann, and E. Sackmann, *Macromol.* **29**, 30 (1996).
- [7] J. Käs, H. Strey, J.X. Tang, D. Finger, R. Ezzell, E. Sackmann, and P.A. Janmey, *Biophys. J.* **70**, 1 (1996).
- [8] K. Kroy and E. Frey, *Phys. Rev. Lett.* **77**, 306 (1996).
- [9] M. Doi and S. F. Edwards, *The Theory of Polymer Dynamics* (Clarendon, Oxford, 1992).
- [10] O. Kratky and G. Porod, *Rec. Trav. Chim.* **68**, 1106 (1949).
- [11] N. Saito, K. Takahashi, and Y. Yunoki, *J. Phys. Soc. Jpn.* **22**, 219 (1967).
- [12] This relation is also obtained from the definition by performing the continuum limit (segment length $s \rightarrow 0$) in a discrete segment model equivalent to a Heisenberg chain, for which ℓ_p is found to be given by $\ell_p = -s/\ln(\coth(\kappa/sk_BT) - sk_BT/\kappa)$ in three dimensional space; see, e.g., M. E. Fisher, *Am. J. Phys.* **32**, 343 (1964).
- [13] S. R. Aragón and R. Pecora, *Macromol.* **18**, 1868 (1985).
- [14] S. R. Aragón, *Macromol.* **24**, 3451 (1991).
- [15] R. A. Harris and J.E. Hearst, *J. Chem. Phys.* **44**, 2595 (1966). R. A. Harris, J.E. Hearst, and E. J. Beals, *Chem. Phys.* **45**, 3106 (1966). R. A. Harris and J.E. Hearst, *J. Chem. Phys.* **46**, 298 (1967).
- [16] J. B. Lagowski, J. Noolandi, and B. Nickel, *J. Chem. Phys.* **95**, 1266 (1991).
- [17] R. G. Winkler, P. Reineker, and L. Harnau, *J. Chem. Phys.* **101**, 8119 (1994).
- [18] L. Harnau, P. Reineker, and R. G. Winkler, *J. Chem. Phys.* **102**, 7750 (1995).
- [19] L. Harnau, R. G. Winkler, and P. Reineker, *J. Chem. Phys.* **104**, 14 (1996). This reference also contains a thorough discussion of the literature.
- [20] J. Wilhelm and E. Frey, *Phys. Rev. Lett.* **77**, 2581 (1996).
- [21] L. Song, U.-S. Kim, J. Wilcoxson, and J. M. Schurr, *Biopolymers* **31**, 547 (1991).
- [22] T. Maeda and S. Fujime, *Macromol.* **17**, 2381 (1984).
- [23] E. Farge and A. C. Maggs, *Macromol.* **26** 5041 (1993).
- [24] K. Kroy *et al.*, (unpublished).
- [25] M. Schmidt and W. H. Stockmayer, *Macromol.* **17**, 509 (1984).
- [26] M. Muthukumar and S. F. Edwards, *Macromol.* **16**, 1475 (1983).
- [27] K. Kroy, Diploma thesis, TU München (1995).
- [28] E. Frey and D. R. Nelson, *J. Phys. I (France)* **1**, 1715 (1991).
- [29] If we had kept the mode number dependence of the mobility, then we would have had to deal with the integral
- $$I(x_m, y) = \int_{x_m}^{\infty} \frac{dx}{x^4} \cos(xy) \left(1 - e^{-2\tilde{\zeta}_{\perp} \tilde{H}_{\perp}(x/x_m L_m) x^4}\right).$$
- However, the corrections to the exponent of the structure factor as found with the effective friction coefficient, Eq. (2.18), are comparable in magnitude to the small deviations arising from other approximations introduced in the main text and are not further analyzed here.
- [30] A contact with a single polymer alone will not represent an effective steric constraint. Hence the actual entanglement length is somewhat longer than the geometric length L_m . Equivalently one could introduce the concept of an effective mesh size which is larger than the corresponding geometric quantity ξ_m . However, in the highly entangled state the two lengths differ merely by a numerical factor.
- [31] M. Tempel, G. Isenberg, and E. Sackmann, *Phys. Rev. E* **54**, 1802 (1996).
- [32] P. A. Janmey, S. Hvidt, J. Käs, D. Lerche, A. Maggs, E. Sackmann, M. Schliwa, and T. P. Stossel, *J. Biol. Chem.* **269**, 32 503 (1994).
- [33] The time scale
- $$t^* = \left(\frac{\Gamma(1/4)}{3\pi\gamma_k^{(0)}}\right)^4 \gamma_k^3 \simeq \tau_{k-1} \propto k^{-4}$$
- for the crossover from the initial decay to the stretched exponential behavior is estimated by equating the two decay laws Eq. (2.18) and Eq. (3.4). For a typical light scattering experiment with actin, t^* lies in the range from 10^1 to $10^2 \mu s$, i.e., the initial slope and the stretched exponential decay can both be measured in such an experiment.
- [34] F. Gittes, B. Mickey, J. Nettleton, and J. Howard, *J. Cell Biol.* **120**, 923 (1993).
- [35] P.-G. de Gennes, *Scaling Concepts in Polymer Physics* (Cornell University Press, Ithaca, 1979).
- [36] A. Bremer, R. C. Milloing, R. Sütterlin, A. Engel, T. D. Pollard, and U. Aebi, *J. Cell Biol.* **115**, 689 (1991).
- [37] E. H. Egelman and R. Padrón, *Nature* **307**, 56 (1984).
- [38] J. Käs, H. Strey, M. Bärmann, and E. Sackmann, *Europhys. Lett.* **21**, 865 (1993).
- [39] F. Ziemann, J. Rädler, and E. Sackmann, *Biophys. J.* **66**, 2210 (1994).
- [40] The problem of lateral confinement in fluorescence microscopic studies was recently analyzed: J. Hendricks, T. Kawakatsu, K. Kawasaki, and W. Zimmermann, *Phys. Rev. E* **51**, 2658 (1995). Moreover, if one of the two degrees of freedom of a polymer in three dimensional

space is projected out by observing only a two dimensional image of the contour, the corresponding variables are no longer independent [J. Wilhelm, (private communication)]. The interpretation of microrheological data is complicated by the fact that the method is neither microscopic nor macroscopic in a strict sense.

APPENDIX

The eigenfunctions of the linear bending equation for the transverse undulations of a weakly bending rod with free ends at $s = \pm L/2$ are given by [13]

$$u(p, s) \propto \frac{\cos \nu_p s/L}{\cos \nu_p/2} + \frac{\cosh \nu_p s/L}{\cosh \nu_p/2}$$

with $\nu_p \approx (2p+1)\pi/2$ for $p > 0$ odd and by the analogue expression with \cos and \cosh replaced by \sin and \sinh , respectively, for p even. Since we will only need the $u(p, s)$ for large $p \gg 1$ and $s \ll L$ (far from the ends), we may drop the hyperbolic terms, which are small of order $\exp(-p\pi/2)$, and write

$$u(p, t) \approx (-)^{(p+1)/2} \cos\left(p\pi \frac{s}{L}\right)$$

for p odd and

$$u(p, t) \approx (-)^{p/2} \sin\left(p\pi \frac{s}{L}\right)$$

for p even. The transverse undulations and forces are expressed as

$$\mathbf{r}_s^\perp(t) = 2 \sum_p \mathbf{r}_p(t) u(p, s), \quad \tilde{\mathbf{f}}_s^\perp = \frac{1}{L} \sum_p \mathbf{f}_p u(p, s).$$

(We do not consider the zero mode.) The mode amplitudes decay as

$$\langle \mathbf{r}_p(t) \mathbf{r}_p(0) \rangle_T = \langle \mathbf{r}_p^2 \rangle_T e^{-t/\tau_p}.$$

Here $\tau_p := \tau_L/p^4$ and $\langle \mathbf{r}_p^2 \rangle_T$ is determined by the equipartition theorem:

$$\langle \mathbf{r}_p^2 \rangle_T = \frac{k_B T L^3}{\kappa (\pi p)^4}.$$

After splitting $\mathcal{R}_{s\zeta}^{\perp 2}(t)$ into dynamic and static contributions

$$\begin{aligned} \mathcal{R}_{s\zeta}^{\perp 2}(t) &= 2 \langle \mathbf{r}_s^\perp(0) \mathbf{r}_\zeta^\perp(0) - \mathbf{r}_s^\perp(t) \mathbf{r}_\zeta^\perp(0) \rangle_T \\ &\quad + \langle (\mathbf{r}_s^\perp(0) - \mathbf{r}_\zeta^\perp(0))^2 \rangle_T, \end{aligned}$$

insertion of the normal modes renders the dynamic term as

$$8 \sum_p \left(\langle \mathbf{r}_p^2 \rangle_T - \langle \mathbf{r}_p(t) \mathbf{r}_p(0) \rangle_T \right) u(p, s) u(p, \zeta).$$

For large p the parentheses are approximately equal for successive terms in the sum and we can then replace the product of eigenfunctions by $\cos(p\pi(s-\zeta)/L)/2$. Substituting the sum for $t \ll \tau_1$ by an integral we arrive at

$$\mathcal{R}_{s\zeta}^{\perp 2}(t) - \mathcal{R}_{s\zeta}^{\perp 2}(0) =$$

$$\frac{4L^3}{\ell_p} \int \frac{dp}{(\pi p)^4} \cos[\pi p(s-\zeta)/L] \left(1 - e^{-t/\tau_p}\right).$$

Introducing the scaling variables as discussed in the main text one now obtains Eq. (2.13).

Finally we derive the initial decay within this approach. In the limit $t \rightarrow 0$, $R_{nm}^\perp(t)$ becomes small. In this case we may expand Eq. (2.8) to first order in $R_{nm}^\perp(t)$. Using Eq. (2.13) and Eq. (2.14) for large $k\xi_m$ and neglecting the static contribution $R_{nm}^\perp(0)$ in the weakly bending rod limit, we get

$$\begin{aligned} g(k, t \rightarrow 0) &= \frac{1}{2} \int_{-1}^1 dx \frac{1}{N} \sum_{nm} e^{ixka(n-m)} \\ &\quad \times \left[1 - (1-x^2) \frac{(\gamma_k t)^{3/4}}{\pi} \int_0^\infty \frac{dz}{z^4} \cos\left(\frac{zka(n-m)}{(t/\tau_{kL})^{1/4}}\right) \right]. \end{aligned}$$

After summation and neglecting $kLx/2$ against $z\phi := zkL/2(t/\tau_{kL})^{1/4}$ we have

$$g(k, t \rightarrow 0) - g(k, 0) =$$

$$\frac{1}{2} \int_{-1}^1 dx (x^2 - 1) \frac{N}{\pi} (\gamma_k t)^{3/4} \int_0^\infty \frac{dz}{z^4} \left(1 - e^{-z^4}\right) \frac{\sin^2 z\phi}{(z\phi)^2}.$$

For short times $t \ll \tau_{kL} \equiv \tau_{k-1}$ (see also [33]) the z -integral reduces to $\pi/2\phi$ and for large scattering vectors $kL \gg 1$ the static structure factor $g(k, 0)$ approaches π/ka , hence

$$\frac{g(k \gg L^{-1}, t \rightarrow 0)}{g(k, 0)} = 1 - \frac{2k_B T}{3\pi \zeta_\perp} k^3 t.$$

The initial decay is simple exponential in time with the initial slope

$$\gamma_k^{(0)} = \frac{k_B T}{6\pi^2 \eta} k^3 \ln(\xi_h/a).$$

A more accurate expression for the initial decay rate is computed in Sec. III. The deviation is due to the approximate treatment of the hydrodynamic interaction in Section II. By comparison of the above result with Eq. (3.4) one can fix the phenomenological parameter ξ_h for rather dilute systems ($k\xi_m \gg 1$), for which hydrodynamic screening is negligible. Then ξ_h becomes roughly equal to the scattering wavelength and no longer has the intuitive physical interpretation of a screening length.